JACS
JOURNAL OF THE AMERICAN CHEMICAL SOCIETY

Article

pubs.acs.org/JACS

Conjugated Polymers with Repeated Sequences of Group 16 Heterocycles Synthesized through Catalyst-Transfer Polycondensation

Chia-Hua Tsai,[‡] Andria Fortney,[‡] Yunyan Qiu, Roberto R. Gil, David Yaron,* Tomasz Kowalewski,* and Kevin J. T. Noonan*

Department of Chemistry, Carnegie Mellon University, 4400 Fifth Avenue, Pittsburgh, Pennsylvania 15213, United States

Supporting Information

ABSTRACT: Periodic π-conjugated polymers of the group 16 heterocycles (furan, thiophene, and selenophene) were synthesized with controlled chain lengths and relatively low dispersities using catalyst-transfer polycondensation. The optical gap and redox potentials of these copolymers were fine-tuned by altering the heterocycle sequence, and atomic force microscopy revealed nanofibrillar morphologies for all the materials. Grazing incidence wide-angle X-ray scattering of the thiophene-selenophene copolymers indicated that the π-stacking distance increased with incorporation of the larger heteroatom (from ~3.7−4.0 Å), while the lamellar spacing decreased (from ~15.8−15.2 Å). The study also revealed that periodic sequences allow electronic properties to be tuned while retaining nanofibrillar morphologies similar to those observed for poly(3-hexylthiophene).

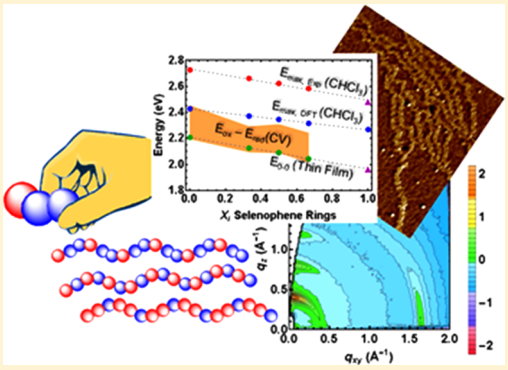

INTRODUCTION

Precise monomer insertion along a polymer backbone allows biological macromolecules to attain a wide range of structural and functional properties. This continues to inspire researchers to synthesize macromolecules while controlling monomer sequence as a means to manipulate the properties of man-made materials.[1] Their efforts are reflected by recent numerous reports demonstrating increasing levels of control over monomer insertion in step-growth and chain-growth polymerization processes.[1] Results of those studies add significantly to understanding the impact of sequence on material properties of polydisperse synthetic polymers.

Sequence control may be especially effective in tuning the electronic properties of conjugated polymers because their electronic structure is highly delocalized.[2] This is manifested in the widely recognized ability to create low band gap polymers by linking electron-rich and electron-poor building blocks to form donor−acceptor copolymers.[3] However, when these building blocks have substantially different shapes, sizes, and polarities, a sequence designed to target a particular optical bandgap or redox potential may lead to unintended consequences on chain packing and material morphology. Such unintended consequences may be minimized through the use of units with similar structures, such as the group 16 heterocycles: thiophene, selenophene, and furan. It is reasonable to expect that the similar shapes of these building blocks will make it possible to vary the sequence without substantially impacting morphology. However, reports of distinct nanoscale phase separation in block copolymers of 3-alkylthiophene and 3-alkylselenophene[4] indicate simple replacement of a heteroatom in the heterocycle may have a significant impact on solid-state packing. Furthermore, while studies of random copolymers of alkylthiophene and alkylselenophene have shown that electronic properties vary smoothly with composition,[5] they also reveal a need to explore the impact of randomness and sequence on solid-state order.

To further elucidate these aspects, in this report we focused on conjugated copolymers with well-defined repeating sequences comprised of 3-hexylthiophene, 3-hexylselenophene, and 3-hexylfuran units. To ensure the sequence is well-defined, the copolymers were synthesized by linking short oligomers through catalyst-transfer polycondensation (CTP).[6] Polymer chains assembled through polycondensation typically grow through a step-growth mechanism, which yields broad molecular weight distributions. CTP on the other hand, proceeds in a chain-growth process, yielding polymers with narrow molecular weight distributions and controlled molecular weights.[6] We demonstrate that, similar to previous reports on random copolymers,[5] the optical bandgaps and redox potentials of the well-defined periodic copolymers vary with composition in a predictable, linear manner. In addition, the periodic sequences exhibit well-defined morphologies, and the packing patterns mimic those of regioregular P3HT, one of the most well-studied semiconducting polymers.

Received: February 20, 2016
Published: April 22, 2016

DOI: 10.1021/jacs.6b01916
J. Am. Chem. Soc. 2016, 138, 6798−6804

RESULTS AND DISCUSSION

The utility of CTP has already been demonstrated with the design of more complex architectures bearing π-conjugated segments including: graft,[7] block,[8] gradient,[4d,9] star,[10] and donor−acceptor polymers.[11] Alternating copolymers have been explored using Kumada CTP,[12] typically with thiophene dimers bearing different side-chain units, but extensions beyond dimers are scarce.[13] In this study, we initially focused on a bithiophene monomer (**1**), to address potential concerns of competitive chain-transfer and termination in CTP of thiophene dimers and trimers.[13]

Monomer **1** was synthesized and activated using 2,2,6,6-tetramethylpiperidinylmagnesium chloride lithium chloride complex (TMPMgCl·LiCl) to selectively deprotonate the 5-position,[14] and polymerization was initiated using Ni(dppp)Cl_2 (Scheme 1). After 15 min, the reaction mixture was quenched,

Scheme 1. Synthesis of Periodic Copolymers

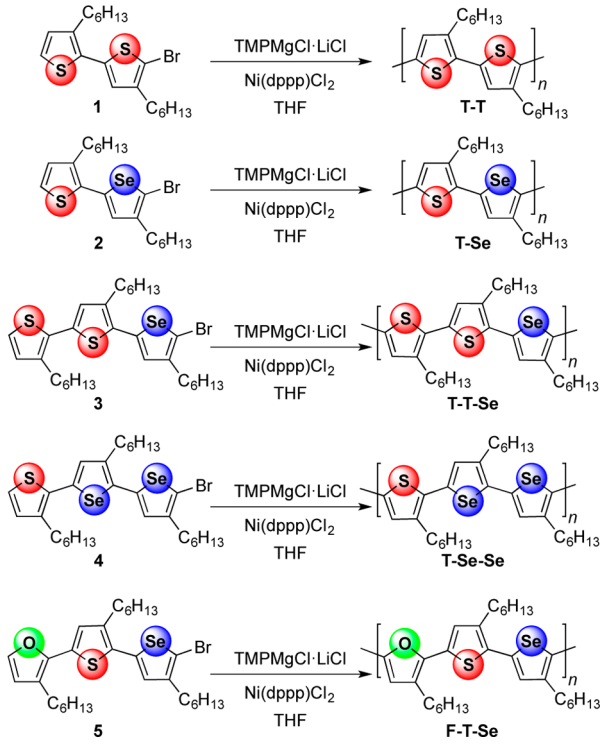

the **T-T** polymer was precipitated with 6 M HCl/MeOH solution and washed with methanol only. We obtained relatively good yields of the final polymer in most cases due to the formation of a single regioisomer as the monomer (Table 1). Gel permeation chromatography (GPC) of the crude polymer samples confirmed excellent control over the molecular weights with relatively low dispersities (Table 1). Although we do observe variation in the molecular weight distribution (in the range of 1.10−1.25) when experiments from Table 1 are repeated, the targeted molecular weights are highly repeatable. The variance in dispersity could be related to catalyst initiation, as McNeil and co-workers have reported large changes in dispersity upon changing the rate of precatalyst initiation.[15]

To build on the success with **1**, monomer **2** was synthesized containing 3-hexylthiophene and 3-hexylselenophene with a head-to-tail (HT) arrangement of the alkyl chains. This perfectly alternating copolymer cannot be obtained by

Table 1. Molecular Weight Data for the Synthesized Polymers

polymer	M/cat.	M_n[a]	$Đ$	yield (%)
T-T	25	12700	1.14	82
	50	27100	1.11	85
	100	36100	1.16	74
T-Se	25	15000	1.16	86
	50	27000	1.11	78
	100	39800	1.18	60
T-T-Se	50	32100	1.23	77
T-Se-Se	50	39000	1.16	83
F-T-Se	50	11700	1.18	42
	100	23100	1.22	30

[a]GPC traces were recorded at 40 °C versus polystyrene standards using THF as the eluent.

combining thiophene and selenophene comonomers in one polymerization, due to the reactivity ratios.[4d] The polymerization of **2** proceeded with excellent control over M_n and low $Đ$, following an identical procedure to that for dimer **1** (**T-Se**, Table 1).

Quenching studies with monomer **2** confirmed deprotonation at the expected position on the thiophene ring and are included in the Supporting Information (Figure S3). The polymerization seemed to be unaffected by the use of a dimeric unit as the monomer, even when the dimeric unit contained two different heterocycles. This suggests the increased chain transfer and termination observed by Kiriy and co-workers in their experiments with thiophene dimers and trimers may have been a consequence of the catalyst (PhNi(PPh_3)$_2$Br) used to initiate polymerization.[13] They postulated that bidendate phosphine nickel catalysts would likely result in improved control, which is consistent with our observations.

The aromatic signals of the **T-Se** polymer main chain appear at 6.92 ppm (H_A, Figure 1) and 7.18 ppm (H_B, Figure 1), corresponding to the thiophene and selenophene ring, respectively. Analysis of this copolymer using 2D NMR spectroscopy led to the assignment of a tail-to-tail (TT) regiodefect at 7.00 ppm (H_C, Figure 1), which results from precatalyst initiation and is similar to the TT defect reported for P3HT.[16] The Br terminated selenophene chain end produced one ^{1}H NMR signal for the ring proton (H_D, Figure 1) and was assigned with the aid of the starting material. The H terminated selenophene end group (H_E, Figure 1) appears at 7.52 ppm and is correlated with a signal at 7.17 ppm (H_F, Figure 1). H_F is only visible in the COSY NMR spectrum, as it overlaps with the major aromatic resonance of the selenophene ring in the polymer main chain (Figure S17, Supporting Information). Integration of the signals for the end groups did not afford the expected 1:1 ratio. MALDI-TOF experiments were attempted to probe this further, but the higher molecular weights limited this analysis. Further studies aimed at exploring the end group fidelity of these TMPMgCl·LiCl activated polymerizations are necessary to explore the end groups in more detail.

Trimers of 3-hexylthiophene and 3-hexylselenophene were synthesized by repeated coupling reactions to afford monomers **3** and **4** (Supporting Information). Polymerization of **3** and **4** produced periodic copolymers with either 33 or 66% selenophene content (**T-T-Se** and **T-Se-Se**). The molecular weight and dispersities were indicative of chain-growth, implying that ring-walking[16b] across three heterocycles is still

DOI: 10.1021/jacs.6b01916
J. Am. Chem. Soc. 2016, 138, 6798−6804

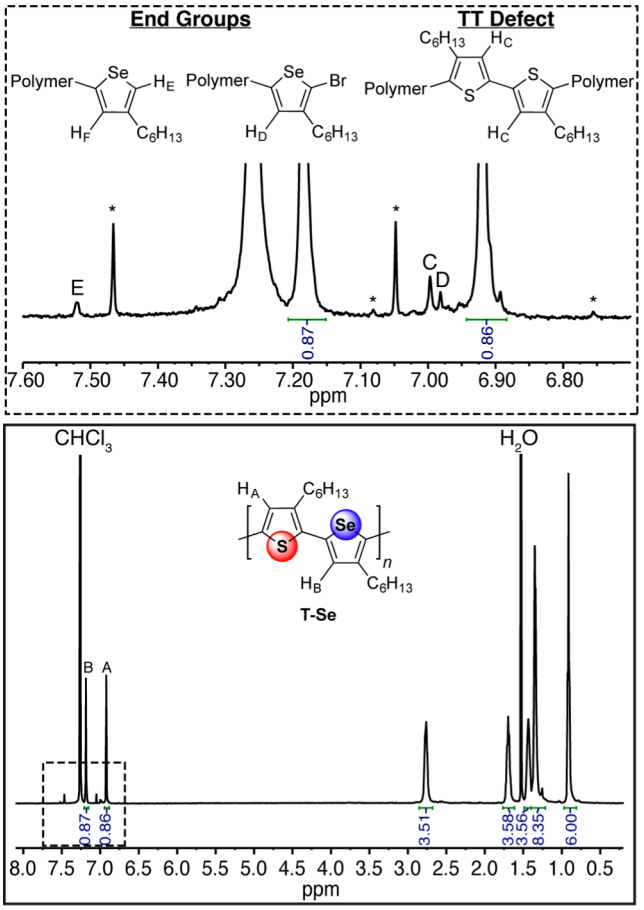

Figure 1. ^{1}H NMR spectrum of the **T-Se** copolymer ($CDCl_3$ at 22 °C). Top panel: expansion of the aromatic region denoted by the dotted square in bottom panel. Aromatic signals for the polymer main chain, TT defect, and end groups are labeled. The star symbols (*) indicate ^{13}C satellite signals for the solvent and polymer.

effective. End group signals in all the thiophene-selenophene copolymers are similar and have been assigned using the **T-Se** copolymer as a reference (Supporting Information). For all the thiophene-selenophene copolymers, the only defect that could be detected using ^{1}H NMR spectroscopy was a TT coupling, which arises precatalyst initiation. In each polymerization, the deprotonation with TMPMgCl·LiCl produces only one active regioisomer as the starting monomer and affords primarily HT coupling, similar to the report on P3HT from Mori and co-workers.[14c,17]

To broaden the scope of sequence control to include a periodic copolymer with three different heterocycles, furan was incorporated into a trimer (monomer **5**, Scheme 1). We recently reported CTP of poly(3-hexylfuran) and demonstrated that furan is amenable to controlled polycondensation when combined in a dimer with thiophene.[18] The periodic copolymer **F-T-Se** was prepared in a similar manner to the others from monomer **5**, but lower yields of the final polymer were obtained (Table 1). The monomer purity for this trimer was more difficult to control, and a small amount of the opposite isomer (Br on the furan and H on the selenophene) was present during the polymerization reaction. The ^{1}H NMR spectrum of **F-T-Se** showed little evidence of defects due to the presence of this isomer during polymerization. Deprotonation of a proton adjacent to an alkyl chain will be difficult using TMPMgCl·LiCl due to steric effects, and the selenophene proton of the minor isomer is adjacent to the hexyl substituent. Mori and co-workers have made a similar observation with 3-hexylthiophene previously.[19]

Analysis of monomer **5** and the **F-T-Se** polymer using ^{1}H coupled HSQC experiments aided in the assignment of the end group signals in the ^{1}H NMR spectrum. A small signal appears at 6.62 ppm, which corresponds to a bifuran TT defect from precatalyst initiation (Figure S24, Supporting Information). The H terminated selenophene end group appears at 7.51 ppm and is again correlated with a small signal at 7.17 ppm. This is almost identical to the end group discussed above for the **T-Se** polymer. The proton for the Br terminated selenophene chain end produced one signal at 6.99 ppm. Some small signals appear near the major aromatic resonance of the thiophene, and we speculate these correspond to the thiophene units near the TT defect and at the end of the polymer chain. It is difficult to completely rule out whether these result from minor defects present along the polymer chain.

The presented results indicate that it is possible to obtain polymers of **F-T-Se** with controlled molecular weights and narrow dispersities. It is of note, however, that polymerizations involving furan containing units proceeded with lower yields and resulted in lower than expected molecular weights.[18] Although the largest oligomer explored by Kiriy and co-workers was terthiophene, they noted that this might not be the limit in controlled polycondensation.[13] To explore this, we also prepared a thiophene tetramer and polymerized it using Ni(dppp)Cl_2. The resultant P3HT (M_n = 25400, $Đ$ = 1.14) is indicative of a well-controlled polymerization, implying that ring walking can extend to four rings. The oligomer length suitable for CTP is clearly dependent on many factors (monomer structure, catalyst structure, additives), and further studies are necessary to probe this behavior in more detail. The polymerization of the tetramer using CTP means larger monomer sequences can potentially be targeted in the controlled synthesis of semiconducting polymers.

The optical properties of all the polymers were probed both in solution and the solid state (Figure 2). The thiophene-

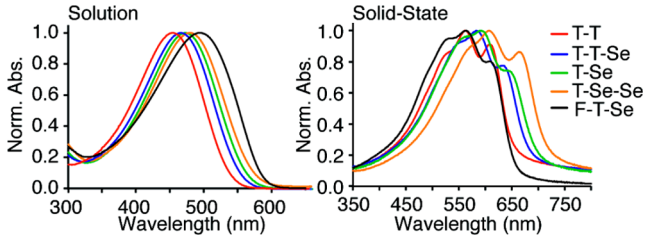

Figure 2. UV–vis absorption spectra recorded in solution ($CHCl_3$) and in the solid state for all the synthesized polymers.

selenophene copolymers display a clear trend, whereby increasing selenophene content results in a red-shifted λ_{max}. The λ_{max} in $CHCl_3$ shifts from 455 nm for **T-T** to 480 nm for the **T-Se-Se** periodic copolymer. While not synthesized here, poly(3-hexylselenophene) continues this trend by exhibiting the most red-shifted absorption of the series (λ_{max} = 499 nm, solution).[20] In the solid state, the thiophene-selenophene systems exhibit the same trend as observed in solution. These results point to a well-controlled bandgap by precise control over the selenophene content in the polymer backbone similar to that observed in the statistical copolymers.[4b,d,e,5] In addition,

DOI: 10.1021/jacs.6b01916
J. Am. Chem. Soc. 2016, 138, 6798–6804

the vibronic structure in the solid-state UV−vis spectrum is well-resolved and indicative of an ordered arrangement.

The **F-T-Se** periodic copolymer has the most red-shifted λ_{max} in solution and the most blue-shifted λ_{max} in the solid state. This is consistent with our previous observations that the smaller furan moiety leads to enhanced planarity in solution.[18] This effect is not present in solid state, where packing forces result in planar π-stacked structures for all the synthesized polymers.

The HOMO−LUMO gap as determined from cyclic voltammetry for the polymer series decreased with increasing molar fraction of selenophene and matched the changes observed for the optical band gap. DFT calculations were performed on oligomers of different sequences and lengths of up to 12 heterocycles. The results are consistent with past work on thiophene and selenophene oligomers, which found twisting of the structures to occur with low energy, both with and without substitutents.[21] Here, we consider planar structures since, in the solid state, packing forces from π-stacking are expected to favor planar configurations. Figure 3 illustrates that

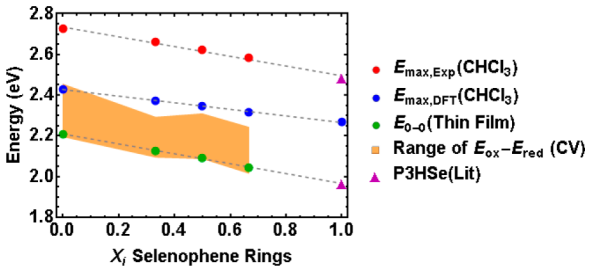

Figure 3. Excitation energies versus Se composition of thiophene-selenophene copolymers from TDDFT (blue), λ_{max} in solution (red), λ_{max} in the solid state (green), and cyclic voltammetry (orange range).

both the experimentally observed excitation energy and that computed using TDDFT on oligomers of length 12 depend linearly on the proportion of selenophene rings. A small disagreement between theory and experiment regarding λ_{max} of the homopolymers leads to somewhat different slopes, but both theory and experiment find a linear dependence on composition.

To gain insight into the origins of this linear dependence, an exciton model was developed in which the excited state is envisioned as containing an exciton that is coherently delocalized along the polymer (Supporting Information).[22] The Hamiltonian matrix for the exciton on an oligomer with N heterocycles is

$$H = \begin{pmatrix} \alpha_1 & \beta & & \\ \beta & \alpha_2 & \ddots & \\ & \ddots & \ddots & \beta \\ & & \beta & \alpha_N \end{pmatrix}$$

where α_i is the energy of the exciton when it resides on site i, with values α_{Se}, α_S, or α_O for selenophene, thiophene, or furan, respectively. These parameters establish the one-dimensional effective energy landscape along which the exciton is coherently delocalized. The coupling between adjacent rings, β, sets the effective mass of the exciton or, equivalently, the energy stabilization due to coherent delocalization of the exciton. The same value, β, is used for all couplings except those involving a furan, which are assigned the value β_O.

Such a model reproduces the TDDFT excitation energy computed for a range of oligomers comprised of between 2 and 12 heterocycles to an accuracy of 0.05 eV. The resulting parameters therefore provide a concise summary of the TDDFT results (α_{Se}: 5.615 eV, α_S: 5.777 eV, α_O: 6.356 eV, β: −1.715 eV, β_O: −1.819 eV). Since the coupling between rings, β, is large compared to the energy differences between heterocycles, the ripples in the energy landscape arising from variations in the sequence have a negligible effect on the wave function describing the exciton delocalization. The exciton thus averages over the heterocycles, causing the excitation energy to depend linearly on the proportion of selenophene versus thiophene units in Figure 3.

AFM images of ultrathin films were prepared by drop-casting from dilute chloroform solutions directly onto silicon substrates (Figures S36 − S40, Supporting Information) with solvent vapor annealing. In all cases, nanofibrillar structures were observed with widths ranging from 24−35 nm, reminiscent of those reported for regioregular P3ATs.[23] In the course of AFM imaging, the surfaces of **F-T-Se** films visibly deteriorated upon rescanning. Optical microscopy of the rescanned regions showed changes that were consistent with photobleaching, as has been observed previously with furan-containing polymers.[18]

The atomic-scale packing was studied using grazing incidence wide angle X-ray scattering (GIWAXS) recorded at the Synchrotron Radiation X-ray Source (CHESS). The gross appearance of 2D GIWAXS patterns (Figure 4) was again similar to the one widely reported for *rr*-P3HT. These studies revealed the presence of out-of-plane reflections (020) originating from π-stacking of polymer backbones along the substrate and in-plane reflections (100) resulting from layering of those π-stacked aggregates parallel to it, with the interlayer spacing dictated by the length of alkyl chains. In all, they showed a clear dependence on the overall content of selenophene rings in the sequence. The average π-stacking and lamellar distances were obtained from the position of Bragg peaks in out-of-plane and in-plane "slices" of 2D GIWAXS patterns, with azimuthal averaging over, respectively, 5−15° and 80−90° (Figure 4). As shown in Figure 4F, the π-stacking distance increased monotonically from 3.7 to 4 Å as the proportion of selenophene rings increased. This can be rationalized in terms of the larger heteroatom, Se versus S, increasing the interchain π-stacking distance. Conversely, the lamellar spacing decreased from 15.8 to 15.2 Å as selenophene content was increased (Figure 4G). In the *rr*-P3AT family this spacing is dictated by the length of the alkyl chains. The decrease with selenophene content may be rationalized in terms of the increase in π-stacking distance, which makes more volume available for side chains between the π-stacks. This increased volume enhances interdigitation of the side chains and contracts the lamellar spacing. Seferos and co-workers have used the alkyl chain length as a tool to match lamellar spacing between 3-alkylthiophenes and 3-alkylselenophenes in random copolymers previously.[24]

Analysis of radial (Figure 4H) and azimuthal (Figure 4I) widths of Bragg peaks in GIWAXS patterns also revealed that the **T-Se** sequence exhibited a considerably higher level of π-stacking and lamellar disorder in comparison with all other sequences. The most likely origin of this disorder for **T-Se** is the curvature of the polymer backbone imparted by the alternation of selenophene and thiophene rings. The curvature

DOI: 10.1021/jacs.6b01916
J. Am. Chem. Soc. 2016, 138, 6798−6804

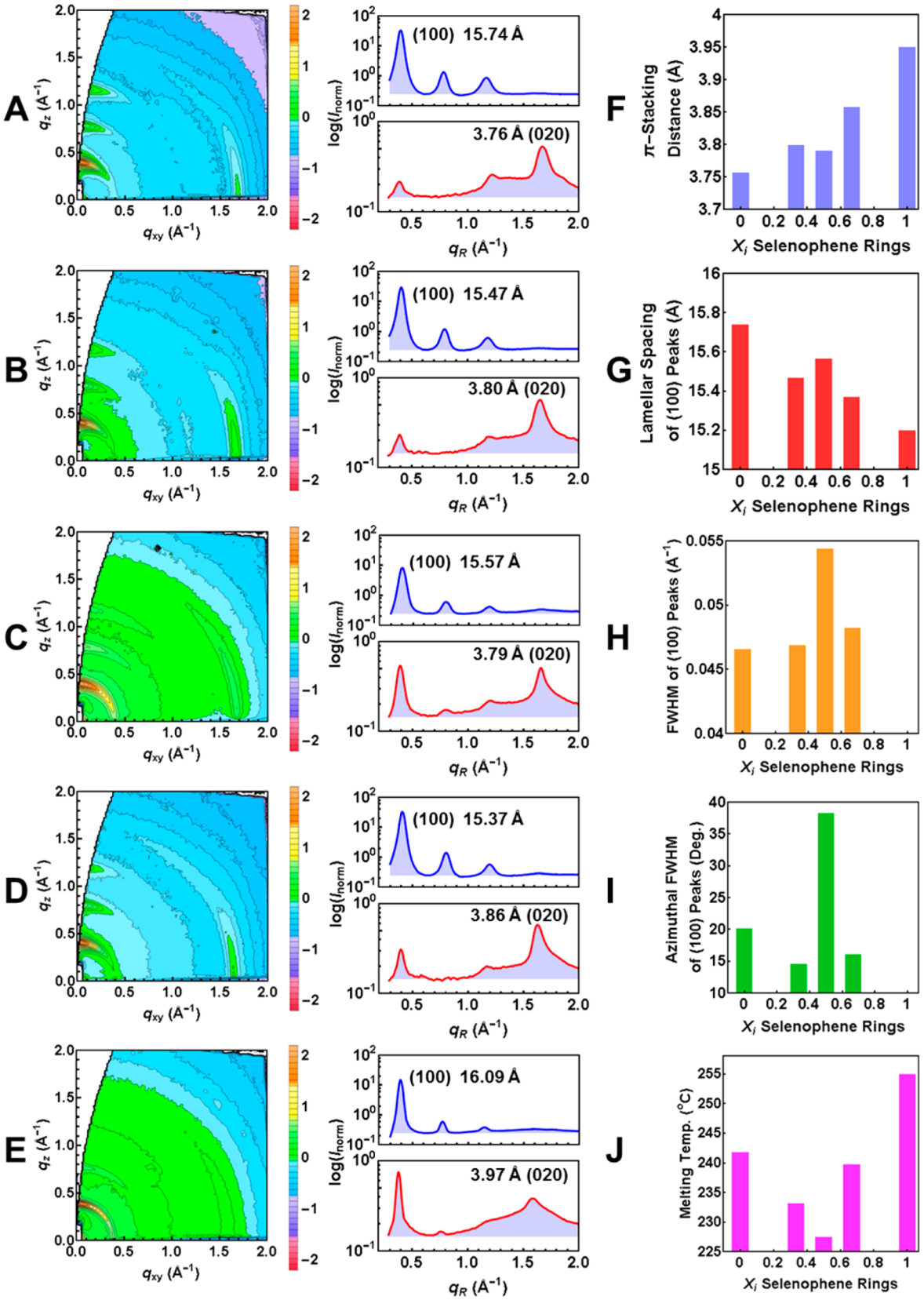

Figure 4. 2D-GIWAXS scattering profiles with scale bar for log of normalized intensity (left), and the azimuthally averaged "slices" of 2D-GIWAXS scattering profiles of in plane (100) (blue) and out of plane (020) (red) Bragg peak reflections (right) for **T-T** (A, M_n = 36100), **T-T-Se** (B, M_n = 32100), **T-Se** (C, M_n = 39800), **T−Se-Se** (D, M_n = 39000), and **F-T-Se** (E, M_n = 23100). π-stacking (F) and lamellar (G) spacing determined from out of plane (020) and in plane (100) Bragg peaks from GIWAXS scattering profiles. The radial (H) and azimuthal (I) full widths at half maxima (fwhm) provide a measure of disorder in the samples that is also reflected in the melting temperatures (J). Data points for Xi = 1 (homopolymer of poly(3-hexylselenophene)) in panels F, G & J originate from reference 20.

DOI: 10.1021/jacs.6b01916
J. Am. Chem. Soc. 2016, 138, 6798−6804

can be traced to the pattern of bond angles along the conjugated backbone (Figure 5). Each of the monomers bends

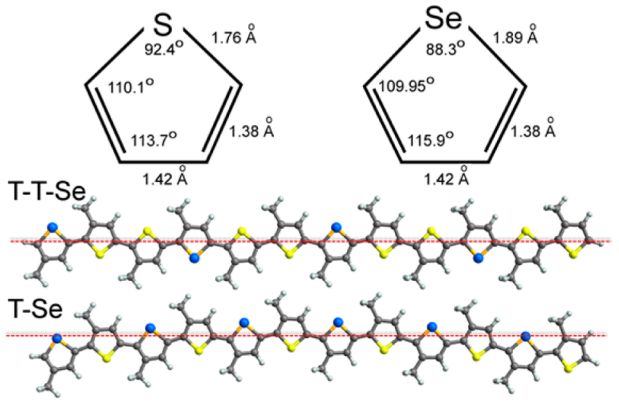

Figure 5. Top: Calculated bond lengths and angles from dodecamer calculations for thiophene and selenophene in the oligomer chain (end groups were excluded). Bottom: Energy minimized **T-T-Se** and **T-Se** dodecamer structures.

the polymer backbone a slightly different amount according to the internal angle determined by the heteroatom bridge (88.3° for Se and 92.4° for S). For the homopolymers, the alternating up/down direction of the monomer ensures the polymer remains overall linear. The same is true for all sequences except the alternating **T-Se** copolymer (Figure 5), which exhibits a curved backbone. Considering that the **T-Se** structure is the only sequence that is expected to have a curved backbone and is the sequence with the largest disorder in the GIWAXS patterns, this strongly implicates the backbone curvature as the source of the disorder in **T-Se.**

The disordered nature of the **T-Se** copolymer is also evident when the differential scanning calorimetry (DSC) traces of all polymers (Figures S41 and S42, Supporting Information) are compared. A distinct lowering of melting temperature (Figure 4J) and heat of fusion (Figure S43, Supporting Information) is observed for the alternating **T-Se** copolymer. Finally, thermogravimetric analysis (TGA) (Figure S44, Supporting Information) points to good thermal stability of all polymers, with an initial decomposition temperature above 339 °C. Notably, the decomposition residue at 600 °C was highest for the P3HT homopolymer, which points to some dependence of carbonization on heteroatom content.

CONCLUSION

In summary, we have designed and synthesized several different sequenced monomers and applied CTP to afford periodic conjugated polymers with controlled molecular weights and relatively low dispersities. The sequences have a predictable impact on the electronic properties of the materials as determined by UV−vis, CV, and computation. Solid-state order of the copolymers was probed using X-ray scattering, DSC, and TGA. These studies indicate that changes in bond lengths from the chalcogen to the diene may introduce curvature in the polymer backbone that can perturb organization. The sequences that mostly closely retain the morphology of P3HT are those for which the repeating sequence retains a linear polymer backbone. Variations in the π-stacking distance were also noted due to changes in heteroatom size, though these do not seem to strongly perturb chain packing. Overall, the incorporation of sequenced monomers offers a means to fine-tune electronic structure while retaining a nanofibrillar morphology. The potential to precisely tune band gaps by controlling the sequence may be valuable when incorporating these systems into organic electronic devices. Further studies will elucidate the impact of randomness on the solid-state organization of group 16 copolymers.

ASSOCIATED CONTENT

Supporting Information

The Supporting Information is available free of charge on the ACS Publications website at DOI: 10.1021/jacs.6b01916.

Complete descriptions of experimental procedures; NMR spectra; GPC traces; CV, DSC, and optical data; and exciton model discussion (PDF)

Optimized molecular geometries and predicted excitation energies (TXT)

AUTHOR INFORMATION

Corresponding Authors

*yaron@andrew.cmu.edu

*tomek@andrew.cmu.edu

*noonan@andrew.cmu.edu

Author Contributions

‡These authors contributed equally.

Notes

The authors declare no competing financial interest.

ACKNOWLEDGMENTS

K.J.T.N. is grateful to the ARO (63038-CH-YIP and W911NF-16-1-0053) and the NSF for a Career Award (CHE-1455136). T.K. gratefully acknowledges financial support from Heinz Endowments (grant no. E1041). NMR Instrumentation at Carnegie Mellon was partially supported by the NSF (CHE-0130903 and CHE-1039870). X-ray scattering results are based partly on research conducted at Cornell High Energy Synchrotron Source (CHESS) which is supported by the National Science Foundation and the National Institutes of Health/National Institute of General Medical Sciences under NSF awards DMR-0936384 and DMR-1332208.

REFERENCES

(1) (a) *Sequence-Controlled Polymers: Synthesis, Self-Assembly, and Properties*; ACS Symposium Series 1170; Lutz, J.-F.; Meyer, T. Y.; Ouchi, M.; Sawamoto, M., Eds.; American Chemical Society: Washington, DC, 2014. (b) Lutz, J.-F.; Ouchi, M.; Liu, D. R.; Sawamoto, M. *Science* **2013**, *341*, 1238149. (c) Lutz, J.-F. *Polym. Chem.* **2010**, *1*, 55−62. (d) Badi, N.; Lutz, J.-F. *Chem. Soc. Rev.* **2009**, *38*, 3383−3390.

(2) Norris, B. N.; Zhang, S.; Campbell, C. M.; Auletta, J. T.; Calvo-Marzal, P.; Hutchison, G. R.; Meyer, T. Y. *Macromolecules* **2013**, *46*, 1384−1392.

(3) (a) Guo, X.; Baumgarten, M.; Müllen, K. *Prog. Polym. Sci.* **2013**, *38*, 1832−1908. (b) Bian, L.; Zhu, E.; Tang, J.; Tang, W.; Zhang, F. *Prog. Polym. Sci.* **2012**, *37*, 1292−1331. (c) Cheng, Y.-J.; Yang, S.-H.; Hsu, C.-S. *Chem. Rev.* **2009**, *109*, 5868−5923.

(4) (a) Hollinger, J.; Seferos, D. S. *Macromolecules* **2014**, *47*, 5002−5009. (b) Gao, D.; Hollinger, J.; Jahnke, A. A.; Seferos, D. S. *J. Mater. Chem. A* **2014**, *2*, 6058−6063. (c) Hollinger, J.; DiCarmine, P. M.; Karl, D.; Seferos, D. S. *Macromolecules* **2012**, *45*, 3772−3778. (d) Palermo, E. F.; McNeil, A. J. *Macromolecules* **2012**, *45*, 5948−5955. (e) Hollinger, J.; Jahnke, A. A.; Coombs, N.; Seferos, D. S. *J. Am. Chem. Soc.* **2010**, *132*, 8546−8547.

(5) (a) Bannock, J. H.; Al-Hashimi, M.; Krishnadasan, S. H.; Halls, J. J. M.; Heeney, M.; de Mello, J. C. *Mater. Horiz.* **2014**, *1*, 214−218.

DOI: 10.1021/jacs.6b01916
J. Am. Chem. Soc. 2016, 138, 6798−6804

(b) Yan, H.; Hollinger, J.; Bridges, C. R.; McKeown, G. R.; Al-Faouri, T.; Seferos, D. S. *Chem. Mater.* **2014**, *26*, 4605−4611.
(6) (a) Yokozawa, T.; Ohta, Y. *Chem. Rev.* **2016**, *116*, 1950−1968. (b) Grisorio, R.; Suranna, G. P. *Polym. Chem.* **2015**, *6*, 7781−7795. (c) Bryan, Z. J.; McNeil, A. J. *Macromolecules* **2013**, *46*, 8395−8405. (d) Kiriy, A.; Senkovskyy, V.; Sommer, M. *Macromol. Rapid Commun.* **2011**, *32*, 1503−1517. (e) Okamoto, K.; Luscombe, C. K. *Polym. Chem.* **2011**, *2*, 2424−2434. (f) Yokozawa, T.; Yokoyama, A. *Chem. Rev.* **2009**, *109*, 5595−5619.
(7) (a) Steverlynck, J.; De Winter, J.; Gerbaux, P.; Lazzaroni, R.; Leclère, P.; Koeckelberghs, G. *Macromolecules* **2015**, *48*, 8789−8796. (b) Zeigler, D. F.; Mazzio, K. A.; Luscombe, C. K. *Macromolecules* **2014**, *47*, 5019−5028. (c) Khanduyeva, N.; Senkovskyy, V.; Beryozkina, T.; Horecha, M.; Stamm, M.; Uhrich, C.; Riede, M.; Leo, K.; Kiriy, A. *J. Am. Chem. Soc.* **2009**, *131*, 153−161.
(8) (a) Verswyvel, M.; Steverlynck, J.; Mohamed, S. H.; Trabelsi, M.; Champagne, B.; Koeckelberghs, G. *Macromolecules* **2014**, *47*, 4668−4675. (b) Willot, P.; Moerman, D.; Leclère, P.; Lazzaroni, R.; Baeten, Y.; Van der Auweraer, M.; Koeckelberghs, G. *Macromolecules* **2014**, *47*, 6671−6678. (c) Erdmann, T.; Back, J.; Tkachov, R.; Ruff, A.; Voit, B.; Ludwigs, S.; Kiriy, A. *Polym. Chem.* **2014**, *5*, 5383−5390. (d) Bhatt, M. P.; Du, J.; Rainbolt, E. A.; Pathiranage, T. M. S. K.; Huang, P.; Reuther, J. F.; Novak, B. M.; Biewer, M. C.; Stefan, M. C. *J. Mater. Chem. A* **2014**, *2*, 16148−16156. (e) Sommer, M.; Komber, H.; Huettner, S.; Mulherin, R.; Kohn, P.; Greenham, N. C.; Huck, W. T. S. *Macromolecules* **2012**, *45*, 4142−4151. (f) Bhatt, M. P.; Huynh, M. K.; Sista, P.; Nguyen, H. Q.; Stefan, M. C. *J. Polym. Sci., Part A: Polym. Chem.* **2012**, *50*, 3086−3094.
(9) (a) Hardeman, T.; Koeckelberghs, G. *Macromolecules* **2015**, *48*, 6987−6993. (b) Palermo, E. F.; McNeil, A. J. Gradient Sequence π-Conjugated Copolymers. In *Sequence-Controlled Polymers: Synthesis, Self-Assembly, and Properties*; ACS Symposium Series 1170; American Chemical Society: Washington, DC, 2014; pp 287−299. (c) Locke, J. R.; McNeil, A. J. *Macromolecules* **2010**, *43*, 8709−8710.
(10) Yuan, M.; Okamoto, K.; Bronstein, H. A.; Luscombe, C. K. *ACS Macro Lett.* **2012**, *1*, 392−395.
(11) (a) Todd, A. D.; Bielawski, C. W. *ACS Macro Lett.* **2015**, *4*, 1254−1258. (b) Senkovskyy, V.; Tkachov, R.; Komber, H.; Sommer, M.; Heuken, M.; Voit, B.; Huck, W. T. S.; Kataev, V.; Petr, A.; Kiriy, A. *J. Am. Chem. Soc.* **2011**, *133*, 19966−19970.
(12) (a) Ono, R. J.; Kang, S.; Bielawski, C. W. *Macromolecules* **2012**, *45*, 2321−2326. (b) Lobez, J. M.; Andrew, T. L.; Bulović, V.; Swager, T. M. *ACS Nano* **2012**, *6*, 3044−3056. (c) Wang, B.; Watt, S.; Hong, M.; Domercq, B.; Sun, R.; Kippelen, B.; Collard, D. M. *Macromolecules* **2008**, *41*, 5156−5165. (d) Benanti, T. L.; Kalaydjian, A.; Venkataraman, D. *Macromolecules* **2008**, *41*, 8312−8315. (e) Hong, X. M.; Tyson, J. C.; Collard, D. M. *Macromolecules* **2000**, *33*, 3502−3504.
(13) Beryozkina, T.; Senkovskyy, V.; Kaul, E.; Kiriy, A. *Macromolecules* **2008**, *41*, 7817−7823.
(14) (a) Tamba, S.; Fuji, K.; Meguro, H.; Okamoto, S.; Tendo, T.; Komobuchi, R.; Sugie, A.; Nishino, T.; Mori, A. *Chem. Lett.* **2013**, *42*, 281−283. (b) Tamba, S.; Mitsuda, S.; Tanaka, F.; Sugie, A.; Mori, A. *Organometallics* **2012**, *31*, 2263−2267. (c) Tamba, S.; Shono, K.; Sugie, A.; Mori, A. *J. Am. Chem. Soc.* **2011**, *133*, 9700−9703. (d) McCullough, R. D.; Lowe, R. D.; Jayaraman, M.; Anderson, D. L. *J. Org. Chem.* **1993**, *58*, 904−912.
(15) Lee, S. R.; Bloom, J. W. G.; Wheeler, S. E.; McNeil, A. J. *Dalton Trans.* **2013**, *42*, 4218−4222.
(16) (a) Kohn, P.; Huettner, S.; Komber, H.; Senkovskyy, V.; Tkachov, R.; Kiriy, A.; Friend, R. H.; Steiner, U.; Huck, W. T. S.; Sommer, J.-U.; Sommer, M. *J. Am. Chem. Soc.* **2012**, *134*, 4790−4805. (b) Tkachov, R.; Senkovskyy, V.; Komber, H.; Sommer, J.-U.; Kiriy, A. *J. Am. Chem. Soc.* **2010**, *132*, 7803−7810. (c) Barbarella, G.; Bongini, A.; Zambianchi, M. *Macromolecules* **1994**, *27*, 3039−3045.
(17) Tamba, S.; Tanaka, S.; Okubo, Y.; Meguro, H.; Okamoto, S.; Mori, A. *Chem. Lett.* **2011**, *40*, 398−399.
(18) Qiu, Y.; Fortney, A.; Tsai, C.-H.; Baker, M. A.; Gil, R. R.; Kowalewski, T.; Noonan, K. J. T. *ACS Macro Lett.* **2016**, *5*, 332−336.
(19) Tanaka, S.; Tamba, S.; Tanaka, D.; Sugie, A.; Mori, A. *J. Am. Chem. Soc.* **2011**, *133*, 16734−16737.
(20) Heeney, M.; Zhang, W.; Crouch, D. J.; Chabinyc, M. L.; Gordeyev, S.; Hamilton, R.; Higgins, S. J.; McCulloch, I.; Skabara, P. J.; Sparrowe, D.; Tierney, S. *Chem. Commun.* **2007**, 5061−5063.
(21) (a) Tsoi, W. C.; James, D. T.; Domingo, E. B.; Kim, J. S.; Al-Hashimi, M.; Murphy, C. E.; Stingelin, N.; Heeney, M.; Kim, J.-S. *ACS Nano* **2012**, *6*, 9646−9656. (b) Zade, S. S.; Zamoshchik, N.; Bendikov, M. *Chem. - Eur. J.* **2009**, *15*, 8613−8624. (c) Zade, S. S.; Bendikov, M. *Chem. - Eur. J.* **2007**, *13*, 3688−3700.
(22) (a) Tozer, O. R.; Barford, W. *J. Chem. Phys.* **2015**, *143*, 084102. (b) Albu, N. M.; Yaron, D. J. *J. Phys. Chem. C* **2013**, *117*, 12299−12306.
(23) Zhang, R.; Li, B.; Iovu, M. C.; Jeffries-EL, M.; Sauvé, G.; Cooper, J.; Jia, S.; Tristram-Nagle, S.; Smilgies, D. M.; Lambeth, D. N.; McCullough, R. D.; Kowalewski, T. *J. Am. Chem. Soc.* **2006**, *128*, 3480−3481.
(24) Hollinger, J.; Sun, J.; Gao, D.; Karl, D.; Seferos, D. S. *Macromol. Rapid Commun.* **2013**, *34*, 437−441.

DOI: 10.1021/jacs.6b01916
J. Am. Chem. Soc. 2016, 138, 6798−6804